Journal of Non-Crystalline Solids 687 (2026) 124149

Contents lists available at ScienceDirect

Journal of Non-Crystalline Solids

journal homepage: www.elsevier.com/locate/jnoncrysol

The role of volume deficiencies in hydrogenated germanium thin films deposited by PECVD for multijunction solar cell fabrication

Paula Perez-Rodriguez *, Devansh Sharma, Shubham Litke, Arno H.M. Smets

Photovoltaic Materials and Devices (PVMD), Delft University of Technology, Mekelweg 4, Delft, Netherlands

ARTICLE INFO

Keywords:
Germanium
PECVD
Solar cells
FTIR

ABSTRACT

Multijunction devices are an effective way to increase the efficiency of solar cell. However, currently only expensive III-V technologies utilize the infrared part of the solar spectrum. To tackle this issue, this work explores the material properties of thin film amorphous hydrogenated germanium deposited by PECVD. It was found that high H_2 dilution rates, deposition temperatures of 275 °C, pressures of 3 to 4 mbar and a power density around 0.20 W/m^2 can achieve films with bandgaps of around 0.9 eV and activation energies above 450 meV, suggesting dense films with intrinsic behaviour. Regarding the mechanisms governing this behaviour, the results suggest that the performance of a-Ge:H is predominantly determined by mid-gap states, which are related to the high mobility of H during deposition within the a-Ge:H matrix. When small amounts of Si are introduced, the H atoms are fixed to the Si, reducing the defect density in the material.

1. Introduction

Multijunction devices are a popular and viable way to increase efficiency of solar cells. Some common examples are III-V technologies [1,2] or, more recently, the perovskite/c-Si tandems [3,4]. However, many of these concepts do not utilize the infrared region of the solar spectrum. To tackle the region of the spectrum between 1200–1500 nm, a low bandgap material could be used [5]. Other possible applications include the use of germanium cells within the thermophotovoltaic field [6]. Germanium can achieve a bandgap of 0.67 eV when fully crystalline, making it an ideal candidate for a bottom cell in a multijunction device. However, crystalline germanium substrates imply a high material use and price [7]. Some efforts have been made to reduce the thickness of the Ge substrates used in these structures [8]. This work proposes an alternative approach by developing a germanium low bandgap thin film to utilize as an absorber for the bottom cell of a multijunction solar cell. Bandgaps between 1–1.3 eV have been reported in literature for thin film germanium films [9–13]. Plasma enhanced chemical vapour deposition (PECVD) is a suitable technique to deposit these thin films and is already used in solar cell production [14–16].

Germanium based thin films are widely used in the semiconductor industry [17,18]. However, the nature of hydrogenated amorphous germanium is relatively unexplored, with only a few studies on the growth of Ge thin films for solar cell applications and the effect of deposition parameters on material characteristics [12,19,10,9]. Moreover, the type of reactor used to make these thin films plays a role on the material characteristics [20,21]. Previous work was done using a counterflow reactor in which the precursor gases are introduced from the side of the reactor [9,10]. In this work, films were made with a PECVD tool using a showerhead configuration, in which the precursor gases are introduced through the electrode. Since the precursors do not need to diffuse in the plasma zone and there is a direct relation between the precursor injection and deposition. This results in more controlled depositions and better-quality films [22,23].

Finally, this work aims at better understanding the material at a nanostructural scale, looking at tail states and band states and how the relate to the optoelectrical properties and metastable defects presents in the material. Moreover, this work addresses the material tissue structure with a detailed FTIR analysis. The nature of the volume deficiencies is determined. Amorphous Ge is known to have more mobile, less stable volume deficiencies during deposition due to the weak bond between Ge and H [19,24]. The effect of temperature is studied to anneal these volume deficiencies out. Moreover, introducing Si as a dopant in these films can give further information on the nature and effect of the volume deficiencies in germanium tissue.

The developed films would allow an improvement on the solar spectrum utilization of all types of multijunction solar cells. The versatility of these materials for integration as a bottom cell on a variety of

* Corresponding author.
E-mail address: p.perezrodriguez-1@tudelft.nl (P. Perez-Rodriguez).

https://doi.org/10.1016/j.jnoncrysol.2026.124149
Received 16 December 2025; Received in revised form 20 April 2026; Accepted 25 April 2026
Available online 7 May 2026

configurations and technologies, including thin film silicon, CIGS, III-V or even perovskite/c-Si devices. Moreover, the deposition via PECVD would allow for easy integration within current industrial techniques while minimizing the material use. Finally, the better understanding of the material would incentivize further developments and optimization of these materials.

2. Materials and methods

The films presented here were simultaneously deposited in Corning XG glass cleaned with acetone and isopropanol; and on n-type Cz polished monocrystalline silicon wafers. Fourier transform infrared (FTIR) spectroscopy and XRD measurements were done on the samples on crystalline silicon wafers. All other measurements were done on the Corning glass samples. The films were made using a multi-chamber Electrorava PECVD tool in a showerhead configuration. The electrode distance was fixed to 10 mm. The precursor gases used were germane (GeH_4), hydrogen (H_2) and silane (SiH_4). Deposition parameters such as pressure, power and substrate temperature were varied during this study.

The films have been characterized using Spectroscopic ellipsometry (SE), Raman spectroscopy, Fourier-transform infrared spectroscopy (FTIR) and photo and dark conductivity measurements. These measurements give a comprehensive idea of the material growth, the optical behaviour and the electrical properties.

Properties such as the optical bandgap, thickness, Urbach energy, refractive index and absorption coefficient were calculated using a J. A. Woollam spectroscopic ellipsometer. The activation energy was measured using an in-house dark conductivity setup. The photoconductivity was measured using a Wacom solar simulator. The FTIR spectra were measured using a Thermo Fisher Nicolet 5700 spectrometer. The amount of low stretching modes (LSM) and high stretching modes (HSM) of a-Ge:H are quantified by fitting a Gaussian to the peaks at 1875 cm^{-1} and 1970 cm^{-1} [25–28], respectively, and normalizing the area below the Gaussian by the thickness of the film. This metric is determined as c_{LSM} or c_{HSM}, which represents the vibrating modes of X-H dipoles, which due to the effective charge and differences of mass translate into the vibrations of the hydrogen atoms. The LSM and HSM have thus been linked to the nature of the vacancies and voids in the material in amorphous silicon [29], and this assumption is extended to amorphous germanium, with a shift in the position of the peaks associated with the change of mass of the dipoles [27,24]. Other tools used for the characterization of the films include a Bruker XRD setup and a Reinshaw inVia Raman spectrometer with a 633 nm laser.

3. Results

a-Ge:H has the potential to be a low bandgap absorber in a multijunction solar cell. The first step towards this goal is to better understand the effect of deposition conditions and material characteristics on the optoelectrical properties. For this purpose, this work first performs a material optimization of amorphous Ge:H deposited by a PECVD on showerhead configuration. Then, we look at the material properties and the underlying physical principles that dominate the optoelectrical properties. Finally, to better understand the nature of the defect present, Si doping is introduced as an intentional dopant.

3.1. Optimization of undoped amorphous Ge:H in showerhead configuration

The main parameters explored in this optimization were substrate temperature, hydrogen dilution, deposition pressure and RF power density.

Effect of substrate temperature. Literature has shown that temperature can significantly affect the properties of a-Ge:H films, especially their density [10]. Fig. 1 shows an agreement with literature,

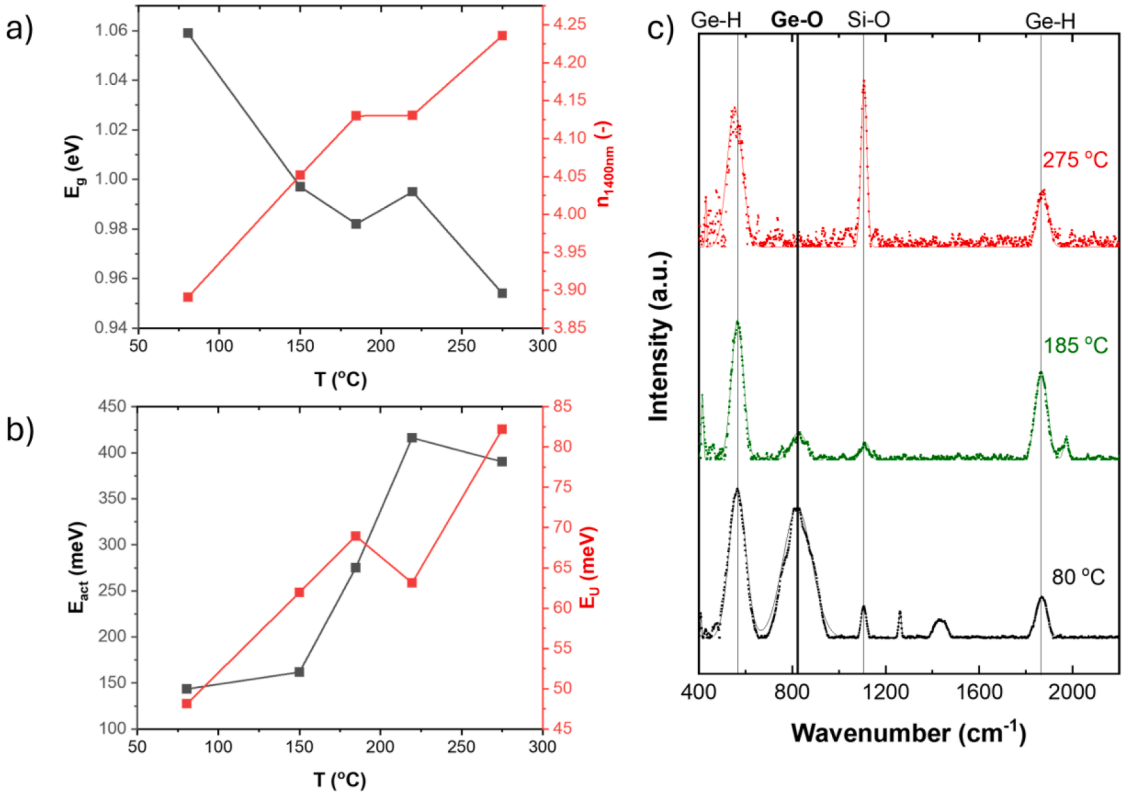

Fig. 1. a) Bandgap, refractive index, Urbach energy and b) activation energy as a function of deposition substrate temperature. c) FTIR spectrum and the fitted peaks at different deposition temperatures (bottom). The peaks were fitted according to [30].

where the optical bandgap is lower at higher deposition temperatures and the refractive index, suggesting higher film densities. In addition, higher temperatures resulted in a higher activation energy, which suggests a more intrinsic, defect-free material. The activation energy shows a plateau at ~220 °C, after which the maximum E_{act} is obtained (~1/2 E_g). This suggests that after that point, further densification of the material does not have a strong impact on the electrical performance, and the limiting factor for activation energy changes after 220 °C. The Urbach energy was also determined to gather more information about the possible defects in the material. The Urbach energy gives an idea of the dangling bonds present within an amorphous lattice, which create band tailing [12]. It can also be understood as the level of amorphicity in a material lattice [29]. The Urbach energy in the samples measured shows a steady increasing trend with substrate temperature, suggesting an increase on the amorphous nature at higher temperatures, potentially due to less inclusion of hydrogen and oxygen bonds within the film, increasing the dangling bonds density. Considering that this does not translate on lower activation energies, the results strongly suggests that dangling bonds are not the main recombination mechanism in the low temperature films. It has been reported that another important advantage of more dense materials achieved by temperature densification is chemical stability and resistance to oxidation [10]. FTIR spectra were measured in as deposited samples at different deposition temperatures (Fig. 1). Incorporated oxygen was detected at lower temperatures, while no germanium-oxygen bond was detected by FTIR at 275 °C. The most likely source of oxidation is post-deposition oxidation, since the PECVD deposition occurs at vacuum in a multi-chamber system, and the process includes a conditioning step pre-deposition that would eliminate any oxygen present in the chamber. Post-deposition oxidation has been shown earlier in Ref [9]. Looking at the stretching modes in the material, there is an increase in the LSM and HSM peaks at higher temperatures, especially at 185 °C. This would suggest that the voids might be too small to accommodate exposure to oxygen or oxygen precursors, but large enough to affect the characteristics of the film. Once the temperature is increased further, these voids become smaller and less prevalent, increasing the density of the film. Overall, considering that a lower bandgap and higher activation energy would be beneficial for a-Ge:H films to be used as a bottom cell absorber, a temperature of 275 °C was used in following experiments.

Effects of hydrogen dilution. Hydrogen could influence the crystallinity of the samples [9], which is also a documented effect for a-Si:H and nc-Si:H samples [31]. In this work, the H_2 flow was kept at 200 sscm, while the GeH_4 was varied between 1 and 5 sccm, resulting in hydrogen dilution fractions between 97.5 and 99.5 %. Fig. 2 shows that the optical performance is reduced at higher dilution rates, with higher bandgap energies and lower absorption coefficients. The density of the material, illustrated by the refractive index (n_{1400nm}), slightly increases at higher dilution rates, but the effect is relatively small. Regarding the electrical properties, the best activation energies are achieved at a dilution rate of 98.5 %, with them significantly degrading at higher dilution ratios. It must be noted that higher dilution ratios result in slightly less controllable and thinner layers, which might explain the worsened optoelectrical properties. Another important parameter to consider is the crystallinity, which might change with hydrogen dilution. From Fig. 2b), it can be seen that for all Raman spectra, no crystallinity peak is seen at 300 cm^{-1}, confirming that in the hydrogen dilution ranges studied do not result on any detectable crystallinity.

Effect of deposition pressure and RF power. The effect of pressure and power are studied jointly since they are interdependent. Fig. 3 shows the effect of both parameters on the bandgap and activation energy. At pressures lower than 2 mbar the plasma did not ignite, at pressures between 2 and 2.5 mbar, there were “islands” of plasma forming, and the bias voltage during deposition was oscillating with amplitudes suggesting dust formation [32]. At pressures higher than 2.5 mbar, the bias voltage becomes stable, avoiding the dust formation regime, and the plasma is also visually stable, not flickering or with “islands” of plasma. Moreover, powers below 0.12 W/cm^2 do not always result in a stable plasma, and therefore the samples at lower pressures and powers could not be characterized electrically. There seems to be a compromise between the stability of the plasma, which is not achieved at pressures below 2–2.5 mbar, and too high pressures resulting in a negative effect on the electrical properties as illustrated by the lower activation energies. A middle ground of 3 to 4 mbar is recommended.

Looking at the effect of deposition power, it does not significantly

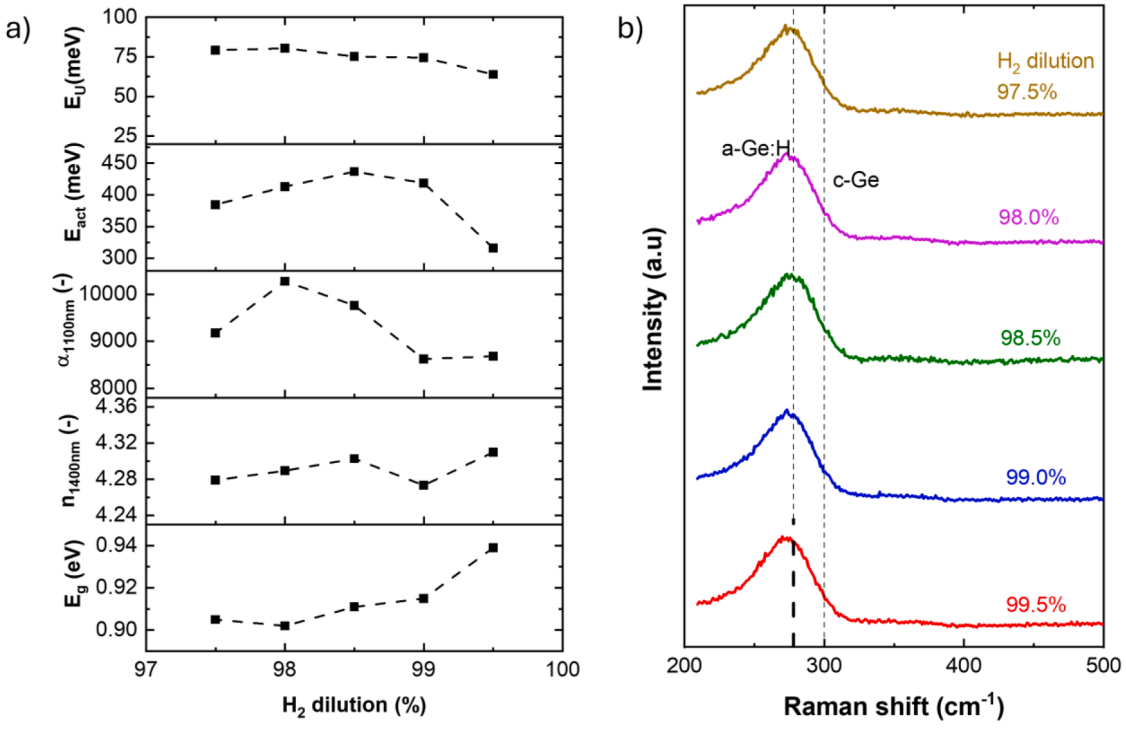

Fig. 2. a) Optoelectrical properties depending on the hydrogen dilution and b) Raman spectrum at different H_2 dilutions.

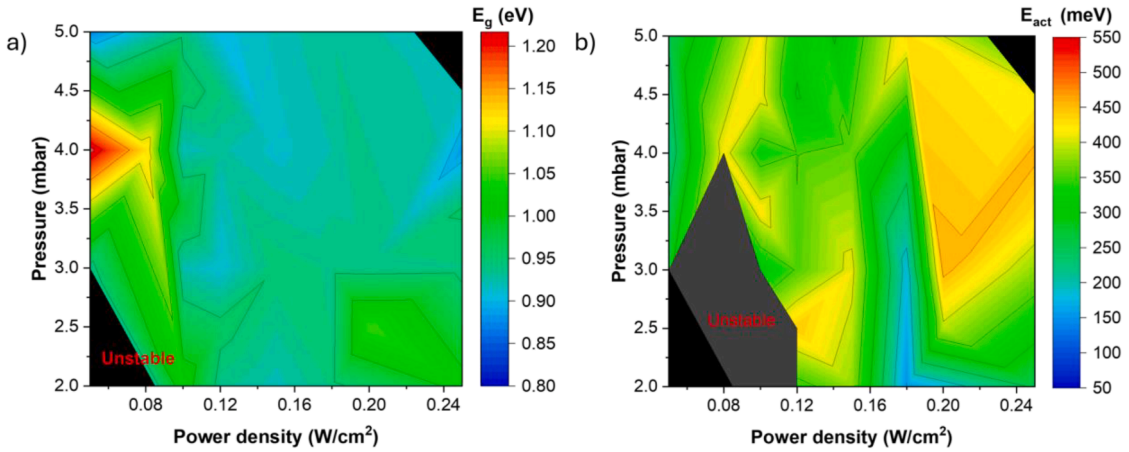

Fig. 3. Dependence of a) bandgap and b) activation energy as a function of deposition power density and pressure.

change when using power densities above 0.12 W/cm^2, being around 0.9–0.95 eV. Electrically, between 0.12 and 0.2 W/cm^2, there are relatively inconsistent results and low activation energies, suggesting the presence of defects in the material that give the material a naturally doped nature. On the other hand, high power densities above 0.2 W/cm^2 result in high activation energies, suggesting that there is enough power to fully dissociate the GeH_4 and form more homogeneous films.

Showerhead vs. counterflow reactor. When comparing the obtained results to previous results achieved by a counter flow reactor configuration [9,10], the achieved materials with showerhead configuration have a much higher deposition rate and more intrinsic behaviour. On the other hand, counterflow reactors can achieve crystalline materials while all the films made with a showerhead reactor during this study were amorphous. These differences could be attributed to the differences in gas residence time within the plasma zone. The residence time in the plasma zone in the showerhead reactor is lower than in the counterflow reactor because the gases are injected directly into the plasma zone. Since the dissociation rate of GeH_4 is very high, the dissociation rate of hydrogen in the plasma zone would be the limiting factor. In the counterflow reactor, the gases are injected in the background and need to diffuse to the plasma zone. Since GeH_4 is a much bigger molecule than H_2, the diffusion of GeH_4 would be the limiting factor for the deposition and could create pressure and gas concentration differences within the plasma zone. As a result, a showerhead reactor allows for higher deposition rates and better control over the GeH_4/H_2 ratio and pressure within the plasma zone, allowing for more intrinsic, potentially better passivated amorphous Ge:H. However, due to the faster deposition and limited H, achieving crystalline conditions might be more challenging [33,34].

3.2. *Volume deficiencies and their effect on the optoelectrical properties*

A wide variety of a-Ge:H films deposited at different powers and pressures were characterized to better understand the material properties and their impact on the optoelectrical behaviour. The films were confirmed to be amorphous both by Raman and XRD measurements (see Supplementary Information). The amorphous films produced have intrinsic behaviour with bandgaps of ~0.9 eV. This study looks further into the nano structure of the material and defect states by looking into the Urbach energy and role of the voids. Urbach energies give information on the H bonding and dangling bond behaviour related to tail states. FTIR measurements can give an idea of the nature of the volume deficiencies inside the material. The Ge-H peak at 550–560 cm^{-1} is associated with wagging modes, whereas the peak at 1875 cm^{-1} is associated with low stretching modes (LSM) of Ge-H and the peak at 1970 cm^{-1} is associated with high stretching modes (HSM) of Ge-H [10]. In amorphous silicon (a-Si:H), LSM have been related to amorphous (di-) vacancies, whereas HSM have been connected to larger vacancies up to nanosized voids [35]. The FTIR measurements of the a-Ge:H samples from this study presented mostly only wagging modes and LSM, indicating that there is not a significant amount of multivacancies or nanovoids. This is in accordance to literature, where it has been shown that RF-PECVD reduces the amount of larger voids present in the case of amorphous silicon films, as the additional energy supplied by the ion induced displacement of surface atom enhances the surface mobility of the silicon or germanium atoms, which move to fill the vacancies during deposition [29]. This would be particularly relevant when depositing germanium films, since the GeH_4 dissociation rate is much higher, and the deposition rate is almost an order of magnitude higher than that of amorphous silicon. Previous studies on a-Ge:H films using a counter flow reactor [10] presented lower deposition rates, higher LSM, and especially higher portion of HSM peaks, suggesting that the showerhead configuration used in this study can reduce the amount of vacancies and nanovoids further.

Fig. 4a and b show the dependence of activation energy to both the LSM modes in the material and the Urbach energy. c_{LSM} is calculated as the area of the FTIR peak LSM Gaussian at 1875 cm^{-1} normalized by the thickness of the film, which gives an idea of the amount of smaller vacancies within the material. The Urbach energy, calculated as Ref. [19], is often associated to the presence of dangling bonds and defect states near the bands that cause band tails [36,37]. According to Fig. 4a, there seems to be a relationship between the activation energy and c_{LSM} when the activation energies are low and deposition rates are low. These results suggest that at low deposition rates, when the plasma is not stable, the volume deficiencies incorporated in the material limit the electrical behaviour. At deposition rates higher than 0.4 nm/s, the LSM volume deficiencies do not seem to be the dominant factor anymore. Once the volume deficiencies have been minimized by increasing the deposition rate, no strong correlation between the activation energy and the nanostructure of the material could be established (LSM, Urbach energy, refractive index, Fig. 4a, b, c). This suggests that once the volume deficiencies are reduced to a threshold level, neither the vacancies nor the amount of dangling bonds are the dominant defect affecting the electrical properties. This might be related with the difficulty of hydrogen inclusion within the germanium films at such high rates.

Literature shows that hydrogen can be difficult to introduce in germanium lattices [38]. This might play a role, where the performance is limited by the dangling bonds. However, data does not show a strong link between band-tail states and the optoelectrical properties, suggesting that the defects present might be at mid-gap. This is supported by the relatively high dark conductivities obtained, despite the intrinsic behaviour achieved (Fig. 4d). However, the overall values have been

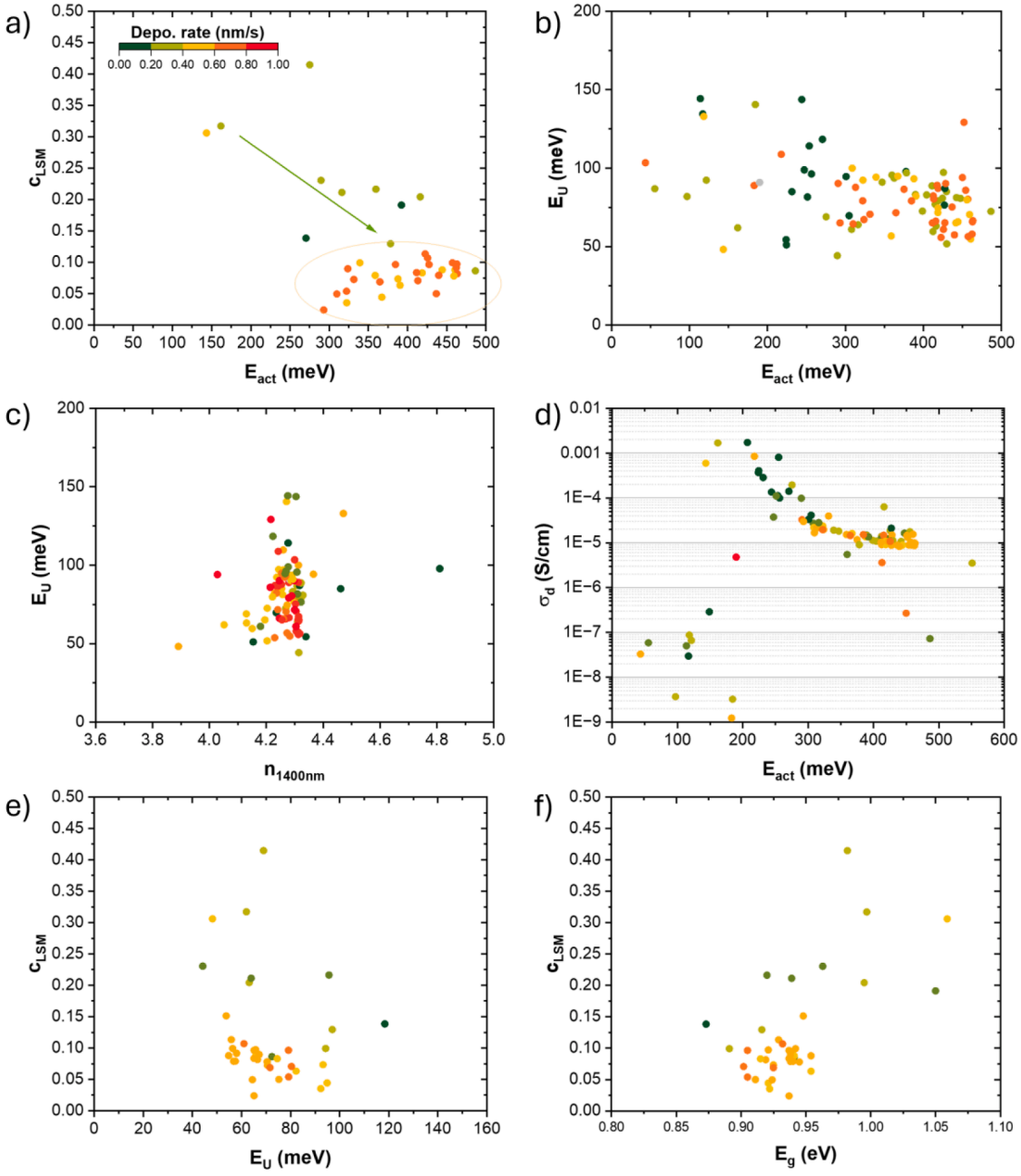

Fig. 4. a) Dependency of activation energy with LSM modes; b) dependency of activation energy with Urbach energy; c) relation between Urbach energy and refractive index at 1400 nm, d) relation between activation energy and dark conductivity, e) Relation between Urbach energy and LSM modes, and f) relation between band gap and LSM modes.

reduced with respect to the samples produced using counterflow reactor, which showed values in the order of 10^{-3} to 10^{-4} S/cm [10]. In Fig. 4d, there is a region at lower activation energies with low deposition rates, where there are many volume deficiencies and the dark conductivity is relatively high. We can conclude that in this region the volume deficiencies are the defects that dominate the electrical properties. When the deposition rate is increased, the dark conductivity saturates, and the activation energy would be dominated by other mechanism, such as the lattice disorder.

Fig. 4e explores the connection between LSM and the tail states, represented by the Urbach energy. In the Ge:H films studied here, volume deficiencies have been annealed out using high temperatures during deposition, there is no oxidation anymore, and the bandgap is reduced by lowering the LSM modes or volume deficiencies. Volume deficiencies put pressure on the tissue, that opens the bandgap. That effect is reduced when vacancies or volume deficiencies are reduced. However, the Urbach energy does not show a clear connection to the LSM states (Fig. 4f), suggesting that a-Ge:H the volume deficiencies do not control the distribution of stress in the lattice, and therefore are not the main mechanism controlling the trends observed in the activation energy.

If we assume that the material behaviour can be comparable to a-Si:H, according to Ref. [29] a lower bandgap is often associated with a decrease in the volumetric compression of the a-Si:H tissue caused by voids. Larger voids (nanovoids or divacancies) result in volumetrically compressed zones, and increase in the band tailing. On the other hand, when dangling bonds are passivated by hydrogen, the bandgap increases. This inverse relationship between bandgap and Urbach energy

has been observed in other materials in literature as well [11,36].

From the analysis performed in these materials, we can conclude that there is a hidden defect mechanism that determines the intrinsic behaviour of the a-Ge:H films, but this mechanism could not be connected to the density of the film, the volume deficiencies present or the Urbach energy. To better understand the effect of hydrogen and mid-gap defects, Si was introduced as a dopant. It is theorized that the volume deficiencies in Ge:H are very mobile during the deposition due to the weak Ge-H bonds. By introducing Si in the lattice, these volume deficiencies are "fixed in place" by the stronger Si-H bond, which allows us to better understand their role in the material.

3.3. The nature of defects in Ge:H and gesi:h

Maintaining all other conditions the same as the previously developed a-Ge:H recipe, a SiH_4 flow was introduced. The Si concentration in the film as measured by EDX shows that introducing SiH_4 linearly increases the Si content from 0 to up to 25 %at. in the flow range studied (See supplementary Information). The resulting optoelectrical and material properties are shown in Fig. 5. Introducing Si in the Ge matrix does increase both the bandgap and activation energy, maintaining the intrinsic behaviour. The dark conductivity is reduced by at least two orders of magnitude with respect to the pure a-Ge:H by introducing silicon. This can be related to the increase in bandgap, but also suggests a decrease in defect density.

Further investigation with FTIR (see Fig. 6) has been conducted to better understand the nanostructure changes in the material. The peak between 500 and 600 cm^{-1}shifts at higher SiH_4. The results suggest that the matrix is changing to accommodate the Si, creating larger voids in the lattice, which are both associated to Ge rich areas and Si rich areas. Hydrogen is more likely to bond with Si than with Ge, therefore reducing the amount of dangling bonds when Si is introduced [39]. These results are in agreement with the overall increase of the wagging mode signature in the FTIR (Fig. 6) between 500–600 cm^{-1}.

Looking at the FTIR results in the region between 1800 and 2100 cm^{-1}, we can gather more information about the nature of the vacancies. The peak at 1860 cm^{-1} is associated with the low stretching modes (LSM) of Ge-H. The peak appearing at 2000 cm^{-1} is associated with the LSM of Si-H. At 6 sccm, there are two peaks appearing at 1940 and 2065cm^{-1}, which correspond to the high stretching modes (HSM) of Ge-H and Si-H, respectively. To better understand the evolution of vacancies as Si is introduced, Gaussian curves were fitted to the LSM and HSM modes, and the areas below them were calculated. Fig. 7 shows the ratio of the gaussian areas of Si-H versus Ge-H for both LSM modes (black) and HSM modes (red). The trend shows that the ratio of Si-H increases with reference to the Ge-H modes, finally arriving to HSM modes to appear. These results suggest that hydrogen shows preferential bonding with Si when compared to Ge, which is in agreement with previous literature [19]. The volume deficiencies are very mobile during deposition in the Ge tissue. This is also suggested by the LSM Ge-H peak, which indicates a change in the Ge-H bonding. The high deposition temperatures anneal the volume deficiencies in the germanium tissue. When Si is present, the hydrogen atoms get fixated on the Si atoms and facilitate a neighbouring volume deficiency. Therefore, introducing Si in the matrix makes the hydrogen atoms and volume deficiencies less

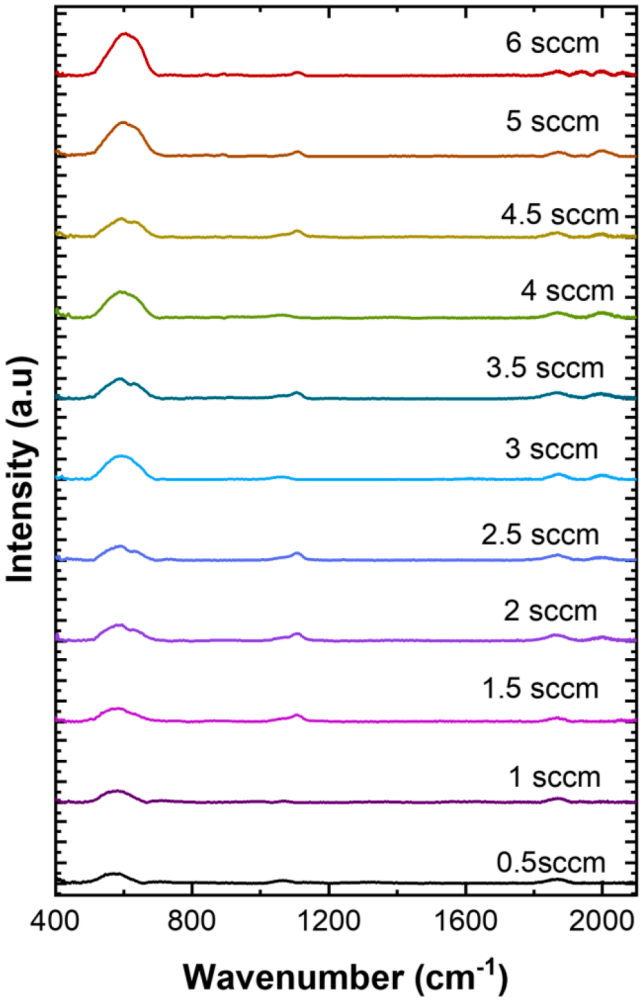

Fig. 6. FTIR analysis of deposited films with different SiH_4 flows.

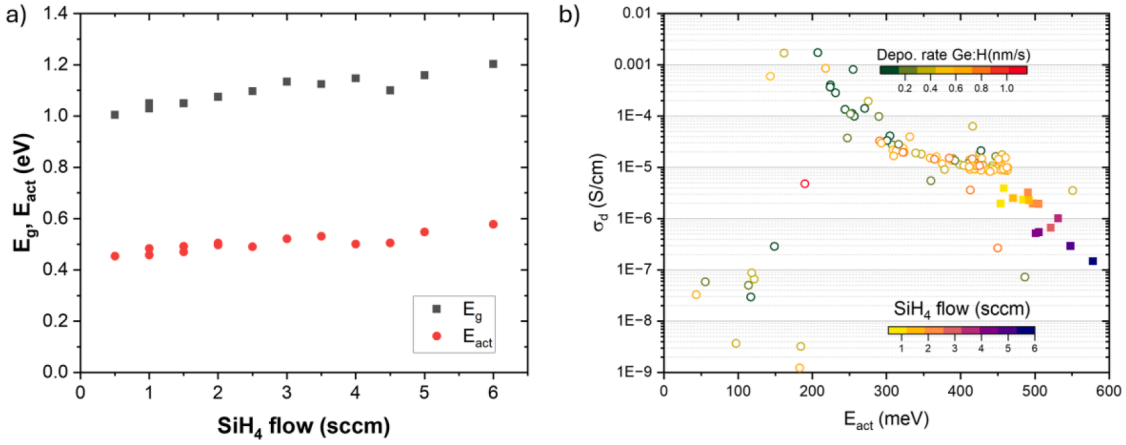

Fig. 5. a) Bandgap and activation energy, and b) dark conductivity as a function of the activation energy and SiH_4 flow.

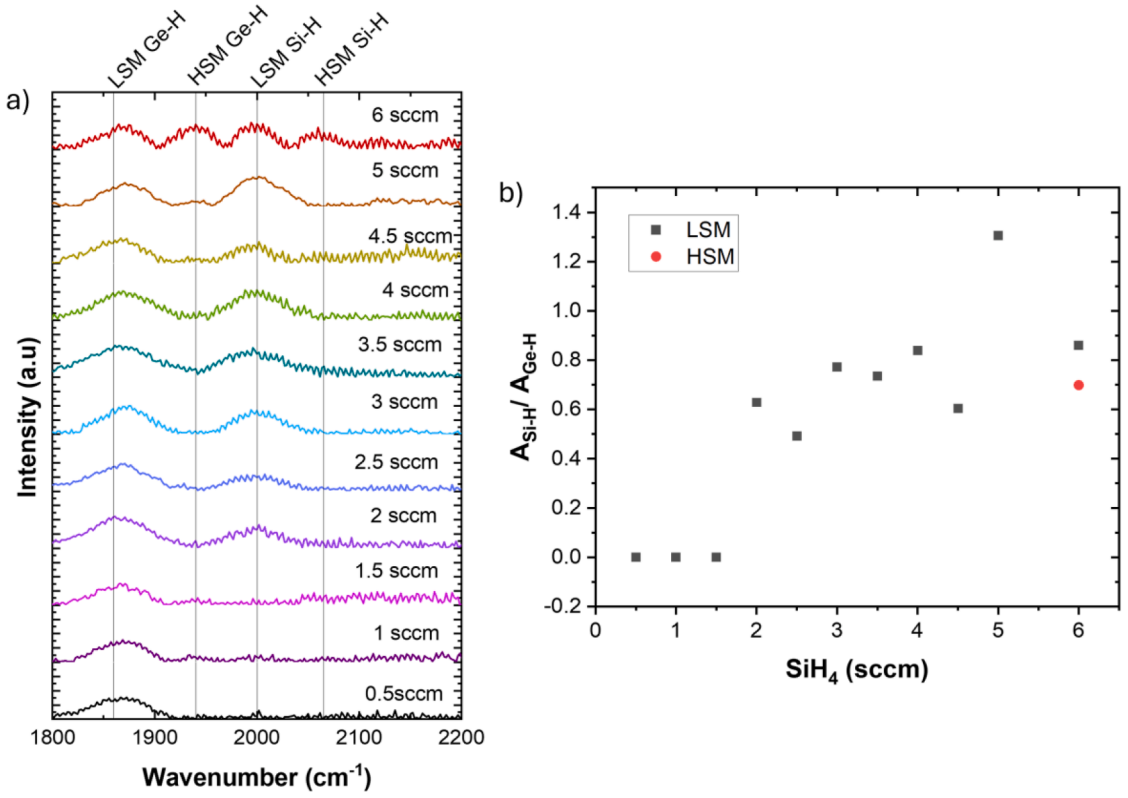

Fig. 7. a) FTIR analysis of the LSM and HSM modes for both Si-H and Ge-H. b) The ratio of the gaussian areas of the Si-H versus Ge-H peaks for both LSM modes (black) and HSM modes (red).

mobile, increasing the passivation in the volume deficiency and consequently within the tissue. That decreases the amount of mid-gap states in the material, which is reflected in the reduction of the dark conductivity as SiH_4 flow increases.

From this analysis, we can suggest that the performance of a-Ge:H is determined by mid-gap states, which are related to mobile H atoms in the matrix and the associated volume deficiencies. When a small amount of Si is introduced, those H atoms are bonded to the Si, becoming less mobile and reducing the defect density in the material, especially relating to the mid-gap states.

4. Discussion and outlook

To determine the overall quality of the material produced in this study, it is interesting to look at the relation between the bandgap and the activation energy, as shown in Fig. 8. Ideally, the activation energy would be about half of the bandgap energy for an intrinsic material (dashed line). Moreover, the bandgap should be as low as possible to accommodate for an effective spectral utilization in a multijunction cell where the a-Ge:H absorber is in the bottom cell. Compared to films previously produced by counterflow reactor (black markers for Ge:H) [9,10], the new films produced during this study (green dots) have a lower bandgap and a more intrinsic behaviour. This is probably due to the lower percentage of large volume deficiencies detected, and the lack of detectable oxidation.

The measured films in this study have a bandgap between 1 and 0.75 eV, which is higher than crystalline germanium (0.67 eV). However, it is important to note that this is still lower than typical values reported in literature for similarly deposited a-Ge:H [10,40]. Since these films are designed to absorb the light in the infrared region, this is a positive development towards that goal. These results show that a showerhead configuration can achieve a more isotropic material with less and smaller vacancies, resulting in a material better suited to be used as a solar cell absorber.

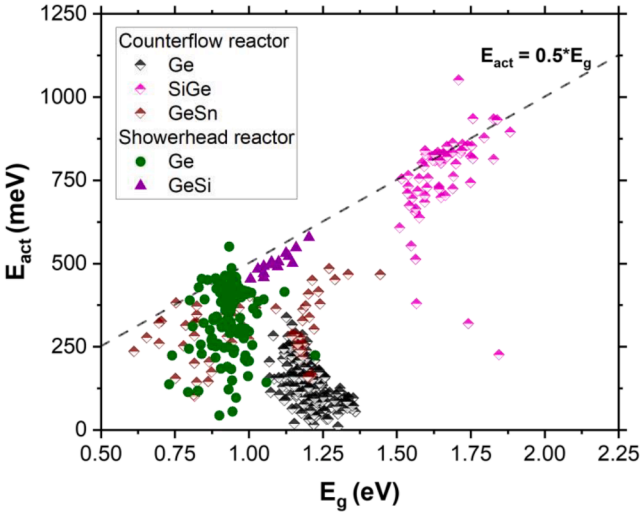

Fig. 8. Relation between bandgap and activation energy as an image of how intrinsic the material is (dotted line). Note that the Background injection data comes from Ref. [10,9,24].

When looking at the effect of doping, the introduction of Si on the a-Ge:H tissue makes the bandgap higher while conserving the intrinsic nature of the material. This could be related to better hydrogen passivation and other changes in the a-Ge:H structure.

5. Conclusions

This research shows that germanium-based films are a promising

absorber material for the bottom cell of multijunction solar cells. Moreover, it shows that PECVD is a suitable technique to fabricate these films. Using this method, bandgaps between 0.75–1 eV are attained. Intrinsic materials are achieved without the need to introduce dopants, with activation energies reaching 450 meV. At higher deposition temperatures the films are densely packed films with, which also makes them chemically stable. The best deposition conditions are established to be at 3–4 mbar, 275 °C and at around 0.20 W/cm^{2,} achieving bandgaps of ~0.9 eV and activation energies of ~450 meV.

When compared with previous films made with a counterflow reactor [10], the showerhead configuration achieves better optical and electrical properties. This is related to the different gas residence times in the plasma zone and the depletion rate of hydrogen.

Looking at the material properties, the performance of a-Ge:H seems to be determined by mid-gap states, which are related to mobile H atoms in the matrix and the associated volume deficiencies. Including Si in the matrix increases the bandgap while maintaining the intrinsic nature. When a small amount of Si is introduced, the H atoms are bonded to the Si, becoming less mobile and reducing the defect density in the material, especially relating to the mid-gap states.

Overall, the achieved properties are compatible with applications as an absorber material in a low-bandgap solar cell. Since these films were produced using PECVD techniques, they can easily be integrated in a solar cell as a proof of concept. Ultimately, they can be integrated as a bottom cell of any of the common multifunction configurations such as perovskite/c-Si, III-V, thin film silicon or CIGS technologies. This will allow for a better spectral utilization in the infrared region, boosting the overall performance of the solar cell with minimal additional processing.

CRediT authorship contribution statement

Paula Perez-Rodriguez: Writing – review & editing, Writing – original draft, Visualization, Validation, Methodology, Investigation, Formal analysis, Data curation, Conceptualization. **Devansh Sharma:** Methodology, Investigation, Formal analysis. **Shubham Litke:** Methodology, Investigation. **Arno H.M. Smets:** Writing – review & editing, Supervision, Resources, Formal analysis.

Declaration of competing interest

The authors declare the following financial interests/personal relationships which may be considered as potential competing interests:

Paula Perez-Rodriguez reports financial support was provided by Hyet Solar B.V. If there are other authors, they declare that they have no known competing financial interests or personal relationships that could have appeared to influence the work reported in this paper.

Acknowledgments

The author acknowledges the financial and technical support provided by the bilateral project between Hyet Solar B.V. and TU Delft.

Supplementary materials

Supplementary material associated with this article can be found, in the online version, at doi:10.1016/j.jnoncrysol.2026.124149.

References

[1] S.P. Philipps, F. Dimroth, A.W. Bett, Chapter I-4-B - high-efficiency III–V multijunction solar cells. McEvoy's Handbook of Photovoltaics, 3rd ed., Academic Press, 2018, pp. 439–472.
[2] J. Li, A. Aierken, Y. Liu, Y.X. Zhuang, H. Yang, J.K. Mo, R.Y. Fan, Q.Y. Chen, S. M. Zhang, Y. Huang, Q. Zhang, A brief review of high efficiency III-V solar cells for space application, Front. Phys. 8 (2021).
[3] J. Yan, T. Savenije, L. Mazzarella, O. Isabella, Progress and challenges on scaling up of perovskite, Sustain. Energy Fuels. 6 (2022) 243.
[4] E. Aydin, T.G. Allen, M.D. Bastiani, A. Razzaq, L. Xu, E. Ugur, J. Liu, S.D. Wolf, Pathways toward commercial perovskite/silicon tandem photovoltaics, Science 383 (2024) eadh3849.
[5] L. Barrutia, I. García, E. Barrigón, M. Ochoa, C. Algora, I. Rey-Stolle, Impact of the III-V/Ge nucleation routine on the performance of high efficiency multijunction solar cells, Sol. Energy Mater. Sol. Cells 207 (2020) 110355.
[6] J. van den Heide, N.E. Posthuma, G. Flamand, W. Geens, J. Poortmans, Cost-effective thermophotovoltaic cells based on germanium substrates, Sol. Energy Mater. Sol. Cells 93 (2009) 1810–1816.
[7] I. Lombardero, N. Miyashita, M. Ochoa, Y. Okada, C. Algora, Thinned germanium substrates for III-V multijunction solar cells, in: *IEEE 46th Photovoltaic Specialists Conference (PVSC)*, 2019. Chicago, IL, USA.
[8] I. Lombardero, L. Cifuentes, M. Gabás, C. Algora, Manufacturing process for III–V multijunction solar cells on germanium substrates with a total thickness below 60 μm, Prog. Photovolt. Res. Appl. 30 (7) (2022) 740–749.
[9] T. de Vrijer, B. Bouazatta, A. Ravichandran, J. van Dingen, P. Roelandschap, K. Roodenburg, S. Roerink, F. Saitta, T. Blackstone, A. Smets, Opto-electrical properties of group IV elements: the challenges of processing hydrogenated germanium, Adv. Sci. (2022) 2200814.
[10] T. de Vrijer, J. van Dingen, P. Roelandschap, K. Roodenburg, A. Smets, Improved PECVD processed hydrogenated germanium films through temperature induced densification, Mater. Sci. Semicond. Process. 138 (2022) 106285.
[11] F.N.C. Anyaegbunam, C. Augustine, A study if optical band gap and associated Urbach energy tail of chemically deposited metal oxides binary thin films, Dig. J. Nanomater. Biostruct. 13 (3) (2018) 847–856.
[12] C. Godet, Improvement of plasma-deposited a-Ge:h thin films by hydrogen dilution of germane, Solid. State Commun. 74 (1990) 721–725.
[13] H. Meddeb, N. Osterthun, M. Gotz, O. Sergeev, K. Gehrke, M. Vehse, C. Agert, Quantum confinement-tunable solar cell based on ultrathin amorphous germanium, Nano Energy 76 (2020) 105048.
[14] F. Duerinckx, J. Szlufcik, Defect passivation of industrial multicrystalline solar cells based on PECVD silicon nitride, Sol. Energy Mater. Sol. Cells 72 (2002) 231–246.
[15] J. Wang, X. Ru, T. Ruan, Y. Hu, Y. Zhang, H. Yan, Performance of heterojunction solar cells with different intrinsic a-Si:h thin layers deposited by RF- and VHF-PECVD, J. Mater. Sci. Mater. Electron. 32 (2021) 25327–25331.
[16] A. Soman, U.K. Das, S.S. Hegedus, Interface engineering by intermediate hydrogen plasma treatment using dc-PECVD for silicon heterojunction solar cells, ACS. Appl. Electron. Mater. 5 (2) (2023) 803–811.
[17] Z. Al-Sharafi, Mohyeddin, S.O. Mohammed, R.M. Kershi, Structural and optical properties of germanium thin films prepared by the vacuum evaporation technique, Phys. Res. Int. (2014) 594968.
[18] E. Wangila, P. Lytvyn, H. Stanchu, C. Gunder, F. de Oliveira, S. Saha, S. Das, N. Eldose, C. Li, M. Zamani-Alavijeh, Growth of germanium thin films on sapphire using molecular beam epitaxy, Crystals 13 (2023) 1557.
[19] C. Godet, Band tails and deep-defect density of states in hydrogenated amorphous germanium, Phys. Rev. B 44 (1991) 5506.
[20] H. Caquineau, B. Despaux, Influence of the reactor design in the case of silicon nitride PECVD, Chem. Eng. Sci. 52 (17) (1997) 2901–2914.
[21] G. Lee, D.K. Sohn, S.H. Seok, H.S. KO, The effect of hole density variation in the PECVD reactor showerhead on the deposition of amorphous carbon layer, Vacuum. 163 (2019) 37–44.
[22] Y.-J. Kim, J.-H. Boo, B. Hong, Y. Kim, Effects of showerhead shapes on the flowfields in a RF-PECVD reactor, Surf. Coat. Technol. 193 (2005) 88–93.
[23] S.-S. Wi, Y.-G. Kim, H.-J. Lee, D. KIm, D. Hwang, W.S. Chang, Effects of showerhead hole structure on the deposition of hydrogenated microcrystalline silicon thin films by vhf PECVD, J. Vac. Sci. Technol. A 30 (2012) 04D113.
[24] T. de Vrijer, B. Bouzatta, A. Smets, Spectroscopic review of hydrogenated, carbonated and oxygenated group IV alloys, Vib. Spectrosc. 121 (2022) 103387.
[25] W. Paul, Structural, optical and photoelectronic properties of improved PECVD a-Ge:H, J. Non. Cryst. Solids. 137&138 (1991) 803–808.
[26] Y.-P. Chou, S.-C. Lee, Structural, optical, and electrical properties of hydrogenated amorphous silicon germanium alloys, J. Appl. Phys. 83 (8) (1998) 4111–4123.
[27] K. Eberhardt, G. Bauer, Effect of H-content and H-bonding configuration on light and thermal induced metastability in amorphous hydrogenated germanium (a-Ge: H), J. Non. Cryst. Solids. 164-166 (1) (1993) 19–22. Vols.
[28] M. Cardona, Vibrational spectra of hydrogen in silicon and germanium, Phys. Status Solidi 118 (2) (1983) 463–481.
[29] A.H.M. Smets, M.A. Wank, B. Vet, M. Fischer, R.A.C.M.M.V. Swaij, M. Zeman, D. C. Bobela, C.R. Wronski, R.M.C.M.V.D. Sanden, The relation between the bandgap and the anisotropic nature of hydrogenated amorphous silicon, IEEE J. Photovolt. 2 (2) (2012) 94–98.
[30] Y.-P. Chou, S.-C. Lee, Evidence for the void size related IR absorption frequency shifts in hydrogenated amorphous germanium films, Solid. State Commun. 113 (2000) 73–75.
[31] T. Itoh, K. Yamamoto, K. Ushikoshi, S. Nonomura, S. Nitta, Characterization and role of hydrogen in nc-Si:H, J. Non. Cryst. Solids. 266-269 (1) (2000) 201–205. Vols.
[32] R.V. Swaaij, B. Girwar, J. Metselaar, Powder formation in germane-silane plasmas, J. Vac. Sci. Technol. A 18 (5) (2000).
[33] M. Abo-Ghazala, S.-A. Hazrny, Hydrogen bonding in hydrogenated amorphous germanium, Tsinghua Sci. Technol. 9 (2) (2004) 177–180.
[34] D. Das, A. Dey, Optimization in the nanostructural evolution of hydrogenated silicon germanium thin film in RF-PECVD, Phys. E: Low-Dimens Syst. Nanostruct. 111 (2019) 20–28.

[35] J. Melskens, A. Smets, S. Eijt, H. Schut, E. Brück, M. Zeman, The nanostructural analysis of hydrogenated silicon films based on positron annihilation studies, J. Non-Cryst. Solids 358 (2012) 2015.
[36] S.J. Ikhmayies, R.N. Ahmad-Bitar, A study of the optical bandgap energy and Urbach tail of spray-deposited CdS:in thin films, J. Mater. Res. Technol. 2 (3) (2013) 221–227.
[37] C. Godet, V. Chu, B. Equer, Y. Bouizem, L. Chahed, I.E. Zawawi, M.L. Theye, S. Basrour, J.C. Bruyere, J.P. Stoquert, Density of states of amorphous germanium thin films deposited by the PECVD of H2-diluted Germane, MRS Online Proc. Libr. 192 (1990) 163–168.
[38] C.V.D. Walle, J. Weber, A. Janotti, Role of hydrogen at germanium/dielectric interfaces, Thin. Solid. Films. 517 (2008) 144–147.
[39] M. Yamaguchi, K. Morigaki, The correlation between hydrogen content and electronic properties in a-Si:H, J. Non. Cryst. Solids. 137-138 (1) (1991) 57–60. Vols.
[40] T. Matsui, C. Chang, T. Takada, M. Isomura, H. Fujiwara, M. Kondo, Thin film solar cells based on microcrystalline silicon–germanium narrow gap absorbers, Sol. Energy Mater. Sol. Cells 93 (2009) 1100.